Ultrathin Layer-by-Layer Hydrogels with Incorporated Gold Nanorods as pH-Sensitive Optical Materials

Veronika Kozlovskaya,[†] Eugenia Kharlampieva,[†] Bishnu P. Khanal,[‡] Pramit Manna,[‡] Eugene R. Zubarev,[‡] and Vladimir V. Tsukruk*,[†]

School of Materials Science and Engineering and School of Polymer, Textile and Fiber Engineering, Georgia Institute of Technology, Atlanta, Georgia 30332, and Department of Chemistry, Rice University, Houston, Texas 77005

Received September 1, 2008. Revised Manuscript Received October 23, 2008

We report ultrathin pH-responsive plasmonic membranes of [poly(methacrylic acid)-gold nanorods]$_{20}$ (PMAA-Au NRs)$_{20}$ with gold nanorods embedded into swollen cross-linked LbL hydrogels. In contrast to the most of known pH responsive materials which rely on pH-triggered change in the intensity of photoluminescence or plasmon bands, the responsive structures suggested here exhibit a significant pH-triggered shift in easily detectable, strong plasmon resonance band. We show that a pH-induced deswelling of the (PMAA-Au NRs)$_{20}$ hydrogel film in the pH change from 8 to 5 causes a dramatic blue-shift of the longitudinal plasmon peak by 21 nm due to the increased side-by-side interactions of adjacent gold nanorods. These composite hydrogel multilayer films can be released from the substrates yielding free-floating and optically pH-responsive ultrathin hydrogel films which can be transferred to the appropriate solid substrates.

Introduction

The unique optical properties of gold nanostructures[1−4] attract a great deal of attention due to their potential applications in organic−inorganic composites[5,6] photonics,[7,8] biomaterials,[9] and biomedicine.[10,11] One of the important properties of gold nanoparticles is the coherent oscillations of the metal electrons in resonance with light of a certain frequency called surface plasmon resonance (SPR) frequency.[12] The intensity and the wavelength of the surface plasmons are highly sensitive to the surrounding environment which can be utilized for sensing purposes via surface enhanced Raman measurements.[13,14] Large enhancement of the electromagnetic field owing to the excitation of the surface plasmons at the particle surface has been intensively studied for sensor applications.[15−18]

On the other hand, stimuli-responsive polymer coatings[19] with adaptive properties such as roughness,[20,21] wettability,[22] biocompatibility,[23] and optical appearance[24] are of great demand for separation,[25] sensing,[26,27]and delivery of functional molecules.[28] It is suggested that embedding metal nanoparticles into polymer matrices is an effective means to combine unique optical properties of gold nanostructures with adaptive behavior of ultrathin membranes enhancing their function as easily hand-able responsive materials.[29] Several related methods have been used for incorporation of spherical gold nanoparticles within the polymer matrix

* To whom correspondence should be addressed. E-mail: vladimir@mse.gatech.edu.
[†] Georgia Institute of Technology.
[‡] Rice University.

(1) Kelly, K. L.; Coronado, E.; Zhao, L. L.; Schatz, G. C. *J. Phys. Chem. B* **2003**, *107*, 668.
(2) Kim, F.; Connor, S.; Song, H.; Kuykendall, T.; Yang, P. *Angew. Chem., Int. Ed.* **2004**, *43*, 3673.
(3) Kumar, P. S.; Pastoriza-Santos, I.; Rodríguez-González, Garcíade Abajo, F. J.; Liz-Marzán, L. M. *Nanotechnology* **2008**, *19*, 015606.
(4) Schwartzberg, A. M.; Zhang, J. Z. *J. Phys. Chem. C* **2008**, *112*, 10323.
(5) Jiang, C.; Markutsya, S.; Tsukruk, V. V. *Langmuir* **2004**, *20*, 882.
(6) Luzinov, I.; Minko, S.; Tsukruk, V. V. *Soft Matter* **2008**, *4*, 714.
(7) Maier, S. A.; Atwater, H. A. *J. Appl. Phys.* **2005**, *98*, 011101/1.
(8) Maier, S. A.; Friedman, M. D.; Barclay, P. E.; Painter, O. *Appl. Phys. Lett.* **2005**, *86*, 071103/1.
(9) Kwon, O.; Kikuchi, A.; Yamato, M.; Sakurai, Y.; Okano, T. *Biomed. Mater. Res.* **2000**, *50*, 82.
(10) Skirtach, A.; Karageorgiev, P.; De Geest, B. G.; Pazos-Perez, N.; Braun, D.; Sukhorukov, G. B. *Adv. Mater.* **2008**, *20*, 506.
(11) Jain, P. K.; Huang, X.; El-Sayed, I. H.; El-Sayed, M. A. *Plasmonics* **2007**, *2*, 107.
(12) Hutter, E.; Fendler, J. H. *Adv. Mater.* **2004**, *16*, 1685.
(13) Stewart, M.; Anderton, C. R.; Thompson, L. B.; Maria, J.; Gray, S. K.; Rogers, J. A.; Nuzzo, R. G. *Chem. Rev.* **2008**, *108*, 494.
(14) Caruso, F.; Spasova, M.; Salguerino-Maceira, V.; Liz-Marzán, L. M. *Adv. Mater.* **2001**, *13*, 1090.
(15) Michaels, A. M.; Nirmal, M.; Brus, L. E. *J. Am. Soc. Chem.* **1999**, *121*, 9932.
(16) Neacsu, C. C.; Dreyer, J.; Behr, N.; Raschke, M. B. *Phys. Rev. B: Condens. Matter* **2006**, *73*, 193406.
(17) Ko, H.; Singamaneni, S.; Tsukruk, V. V. *Small* **2008**, *4*, 1576.
(18) Jiang, C.; Lio, W. Y.; Tsukruk, V. V. *Phys. Rev. Lett.* **2005**, *95*, 115503.
(19) Luzinov, I.; Minko, S.; Tsukruk, V. V. *Prog. Polym. Sci.* **2004**, *29*, 635.
(20) Lupitskyy, R.; Roiter, Y.; Tsitsilianis, C.; Minko, S. *Langmuir* **2005**, *21*, 8591.
(21) Sidorenko, A.; Krupenkin, T.; Taylor, A.; Fratzl, P.; Aizenberg, J. *Science* **2007**, *315*, 487.
(22) Sidorenko, A.; Krupenkin, T.; Aizenberg, J. *J. Mater. Chem.* **2008**, *18*, 3841.
(23) Krsko, P.; Libera, M. *Materials Today* **2005**, *8*, 36, and references therein.
(24) Houbenov, N.; Minko, S.; Stamm, M. *Macromolecules* **2003**, *36*, 5897.
(25) Bruening, M. L.; Dotzauer, D. M.; Jain, P.; Ouyang, L.; Baker, G. L. *Langmuir* **2008**, *24*, 7663.
(26) Caruso, F.; Spasova, M.; Susha, A.; Giersig, M.; Caruso, R. A. *Chem. Mater.* **2001**, *13*, 109.
(27) Cameron, A.; Shakesheff, K. M. *Adv. Mater.* **2006**, *18*, 3321.
(28) Ganta, S.; Devalapally, H.; Shahiwala, A.; Amiji, M. *J. Controlled Release* **2008**, *126*, 187.
(29) Jiang, C.; Tsukruk, V. V. *Soft Matter* **2005**, *1*, 334.

10.1021/cm8023633 CCC: $40.75 © 2008 American Chemical Society
Published on Web 11/26/2008

including Langmuir−Blodgett deposition,[30,31] electrostatic[32] and hydrogen-bonded self-assembly.[33] Most of the methods rely on the preassembly modification of particles surfaces with ligands capable of strong noncovalent interactions with polymers used for the layer-by-layer (LbL) deposition.[34,35]

For instance, Minko and co-workers have recently reported on a nanosensor based on brushes of poly(2-vinyl pyridine) (P2VP) with citrate-stabilized spherical gold nanoparticles adsorbed on top of the brushes.[36] Interactions of adsorbed gold nanoparticles with gold nanoislands precoated on the glass surface were triggered by pH-induced shrinking of the brushes in the pH range from 2 to 5. More recently, they demonstrated that specifically designed pores on P2VP gel can be decorated with gold nanospheres. pH-controlled interactions of the nanoislands preformed on the glass surface with the Au nanospheres along the P2VP gel pores caused large shifts in the absorption maximum.[37] Similar approach has been used for the preparation of freely floating nanoparticle sensing devices.[38] In that work, citrate-stabilized gold nanoparticles were directly immobilized on P2VP chains grafted to silica nanoparticles. The reversible red-shift of the absorption band by 13 nm was demonstrated when pH of the modified silica nanoparticles was varied in the range between 2 and 5. The fabrication of molecularly imprinted polymer gels on a gold substrate with gel-embedded gold nanoparticles showing enhancement in signal intensity (change in SPR angle) due to gel swelling upon dopamine binding was also reported.[39] A combination of nanowires and nanoparticles designed to tune a SPR band position in the presence of selective analytes has been reported by Kotov et al.[40]

The LbL films were widely used to study optical properties of noble metal nanoparticles embedded within the polymer matrices.[5] A strong effect of interparticle distance on the surface plasmon absorption of Au nanoparticles has been reported.[41] Gold nanoparticles were also used to enhance SPR signal under attenuated total reflection (ATR) spectroscopy conditions[42] in LbL films made from poly(allylamine hydrochloride)/polystyrene sulfonate (PAH/PSS) and Au NPs and deposited on gold- or silver-coated substrates. Moreover, gold nanorods exhibit more attractive optical properties as compared to nanospheres due to anisotropic shape. There are two major absorption bands in the electromagnetic spectrum of the nanorods: the wavelength maximum centered at ∼520 nm corresponds to the transverse plasmon oscillations of nanorods. It depends on the aspect ratio and the diameter of the rods. The second adsorption maximum around 700−800 nm is due to the longitudinal plasmon oscillations and possesses much stronger intensity and can be tuned by varying the length of the nanorods.[43] To date, these unique SPR properties have not been utilized in responsive nanomaterials.

It is worth noting that for practical applications it is important to be able to fabricate films which can be later transferred to various substrates.[44,45] This option is important because such free-standing films offer a faster response and permeability due to their low thickness and the absence of substrate as well as versatility in integration with various microfabricated substrates. The LbL method on sacrificial substrates was widely used to fabricate free-standing polymer films with inorganic particles for the improvement of their mechanical properties.[46−49] The spin-assisted LbL assembly[50] in contrast to the dip-assisted LbL technique offers the advantages of much shorter fabrication times and firm control over the bilayer thickness as well as the surface properties of the produced films.

In this work, we report on the preparation of pH-responsive ultrathin plasmonic LbL membranes of (PMAA-Au NRs)$_{20}$ via postinclusion of Au nanorods into highly swollen (PMAA)$_{20}$ layered hydrogel films. These films showed dramatic pH response as readily detected and very significant shift (more than 20 nm) in an easily detectable plasmon band position in contrast with most of pH-responsive structures known to date which rely on rather ambiguous detection of modest changes in the intensity of the photoluminescence or plasmon bands.

The PMAA films were synthesized via chemical cross-linking of hydrogen-bonded (poly(*N*-vinylpyrrolidone)/PMAA)$_{20}$, (PVPON/PMAA)$_{20}$, films with ethylenediamine (EDA). There is just one major example on spin-assisted LbL assembly (SA-LbL) of hydrogen-bonded layers in the literature,[51] and here, we extend the knowledge on the hydrogen-bonded deposition using a SA-LbL method and demonstrate that thinner LbL films are produced from dilute concentrations of polymer solutions as compared to those formed by dip-coating LbL. We also show that the longitudinal plasmon peak from (PMAA-Au NRs)$_{20}$ hydrogel films reversibly shifts to lower wavelengths in response to pH change from 8 to 5 (and back) due to deswelling of the film resulting in stronger interactions of the gold nanorods.

(30) Chen, S. *Langmuir* **2001**, *17*, 2878.
(31) Endo, H.; Mitsuishi, M.; Miyashita, T. *J. Mater. Chem.* **2008**, *18*, 1302.
(32) Jiang, C. Y.; Markutsya, S.; Shulha, S.; Tsukruk, V. V. *Adv. Mater.* **2005**, *17*, 1669.
(33) Hao, E.; Lian, T. *Chem. Mater.* **2000**, *12*, 3392.
(34) *Multilayer Thin Films* Decher, G., Schlenoff, J. B., Eds.; Wiley-VCH: Weinheim, 2003.
(35) Lvov, Y.; Decher, G.; Möhwald, H. *Langmuir* **1993**, *9*, 481.
(36) Tokareva, I.; Minko, S.; Fendler, J. H.; Hutter, E. *J. Am. Chem. Soc.* **2004**, *126*, 15950.
(37) Tokarev, I.; Tokareva, I.; Minko, S. *Adv. Mater.* **2008**, *9999*, 1.
(38) Lupitskyy, R.; Motornov, M.; Minko, S. *Langmuir* **2008**, *24*, 8976.
(39) Matsui, J.; Akamatsu, K.; Hara, N.; Miyoshi, D.; Hawafune, H.; Tamaki, K.; Sugimoto, N. *Anal. Chem.* **2005**, *77*, 4282.
(40) Lee, J.; Hernandez, P.; Lee, Jun.; Govorov, A.; Kotov, N. A. *Nat. Mater.* **2007**, *6*, 291.
(41) Malikova, N.; Pastoriza-Santos, I.; Schierhorn, M.; Kotov, N. A.; Liz-Marzan, L. *Langmuir* **2002**, *18*, 3694.
(42) Jiang, G.; Baba, A.; Ikarashi, H.; Xu, R.; Locklin, J.; Kashif, K. R.; Shinbo, K.; Kato, K.; Kaneko, F.; Advincula, R. *J. Phys. Chem. C* **2007**, *111*, 18687.
(43) Jana, N. R.; Gearheart, L.; Murthy, C. J. *Adv. Mater.* **2001**, *13*, 1389.
(44) Jiang, C. Y.; Tsukruk, V. V. *Adv. Mater.* **2006**, *18*, 829.
(45) Miller, L. L.; Zhong, C. J.; Kasai, P. *J. Am. Chem. Soc.* **1993**, *115*, 5982.
(46) Jiang, C. Y.; Markutsya, S.; Pikus, Y.; Tsukruk, V. V. *Nat. Mater.* **2004**, *3*, 721.
(47) Lutkenhaus, J. L.; Hrabak, K. D.; McEnnis, K.; Hammond, P. T. *J. Am. Chem. Soc.* **2005**, *127*, 17228.
(48) Mamedov, A. A.; Kotov, N. A.; Prato, M.; Guldi, D. M.; Wicksted, J. P.; Hirsh, A. *Nat. Mater.* **2002**, *1*, 190.
(49) Tang, Z. Y.; Kotov, N. A.; Magonov, S.; Ozturk, B. *Nat. Mater.* **2003**, *2*, 413.
(50) Cho, J.; Char, K.; Hong, J.; Lee, K. *Adv. Mater.* **2001**, *13*, 1076.
(51) Seo, J.; Lutkenhaus, J. K.; Kim, J.; Hammond, P. T.; Char, K. *Langmuir* **2008**, *24*, 995.

In contrast to previously reported systems, these films do not require substrate precoating with gold or silver and can be released as free-floating films transferrable to any appropriate substrate. To the best of our knowledge, this is the first example when gold nanorods as opposed to spherical particles are used in combination with pH-responsive layered films thus facilitating very significant and easily detectable shift in longitudinal plasmon bands.

Experimental Section

Materials. Poly(allylamine hydrochloride) (PAH, $M_w = 70$ kDa), poly(methacrylic acid) (PMAA, $M_w = 150$ kDa), poly(N-vinylpyrrolidone) (PVPON, $M_w = 55$ kDa), mono- and dibasic sodium phosphate 1-ethyl-3-(3-dimethylaminopropyl) carbodiimide hydrochloride (EDC), *N*-hydroxy-sulfosuccinimide sodium salt (NSS), hexadecyltrimethylammonium bromide (CTAB), EDA, and $HAuCl_4$ solution were purchased from Sigma-Aldrich. Ultrapure (Nanopure system) filtered water with a resistivity 18.2 MΩ cm was used in all experiments. Quartz microscope fused slides (Alfa Aesar) and single-side polished silicon wafers of the {100} orientation (Semiconductor Processing Co.) were cut by typical size of 10 × 20 mm and cleaned in a piranha solution as described elsewhere.[52]

Synthesis of Gold Nanorods. To prepare a seed solution, 364 mg of CTAB was dissolved in 5 mL of water upon a slight heating with a heat gun (up to 30−35 °C). In a separate vial, 1 mg of $HAuCl_4 \times 3\ H_2O$ was dissolved in 5 mL of water at room temperature. The two solutions were mixed together right after their preparation and 0.6 mL of 0.01 M ice-cold aqueous solution of $NaBH_4$ was added at once upon vigorous stirring (1200 rpm). Upon the color change from greenish-yellow to brown the mixture was stirred for 2 min. The stirring was stopped and the seed solution containing 2 nm Au nanoparticles stabilized by CTAB surfactant was used 5 min after the stirring was stopped.

Au nanorods stabilized by CTAB surfactant were prepared using a modified seed-mediated growth method as reported in literature.[43,53,54] To grow gold nanorods, 8.5 mg of $AgNO_3$ was dissolved in 12.5 mL of water. A total of 18.22 g of CTAB was dissolved in 250 mL of water in a 500 mL Erlenmeyer flask. In order to completely dissolve the CTAB, a slight heating with a heat gun was used. The two solutions were mixed and the mixture was kept at 25 °C (oil bath) without any stirring. After 10 min, 250 mL of aqueous solution of $HAuCl_4 \times 3\ H_2O$ (prepared separately by dissolving 98.5 mg in 250 mL of H_2O) was added to the aqueous solution of CTAB and $AgNO_3$. After 3 min, 3.5 mL of 0.0788 M aqueous solution of ascorbic acid was added to the above mixture. The flask was hand-stirred until the mixture became colorless. The obtained growth solution was used right after its preparation. At this point, 0.8 mL of seed solution was added to the entire growth solution (∼535 mL) and the mixture was stirred for 30 s. Next, the flask containing the growth solution was placed into an oil bath at 27 °C and kept without stirring. A reddish-brown color slowly developed within the first 10 min.

Fabrication and Release of Hydrogel-Au NRs Films. Hydrogen-bonded films of $(PMAA/PVPON)_{20}$ were deposited through SA-LbL method according to the reported procedure.[49] To enhance the surface adhesion of the subsequently grown multilayer as well as the swollen hydrogel films, three bilayers of PAH/PMAA precursors were first spin-cast onto the substrates starting from 0.5 mg/mL PAH solution. The precursor layers were heated to 125 °C for 1 h in an oven for thermal cross-linking of $(PAH/PMAA)_3$ layers and their enhanced adhesion to the substrate surfaces.[55] We utilized these precursor-treated quartz microslides or silicon wafers for deposition of hydrogen-bonded (PMAA/PVPON) multilayers. Specifically, 0.2, 0.5, or 1.0 mg/mL polymer solutions were spin-cast onto the substrates and rotated at 4000 rpm for approximately 20 s starting from PVPON if deposition was performed on the substrates without prelayers and if the pretreated substrates were employed.

After hydrogen-bonded multilayers were formed, they were chemically cross-linked with EDA as has been developed in previous studies and described in detail elsewhere.[56,57] Briefly, PAH/PMAA-tethered $(PVPON/PMAA)_{20}$ films were immersed into solution of EDC and NSS at pH 5 for 30 min to activate the carboxylic groups of PMAA and then transferred into 5 mg/mL EDA solution at pH 5 for 20 h to introduce amide linkages between EDA molecules and the activated carboxylic groups. After the cross-linking reaction was completed, the substrates with tethered hydrogel films were immersed in a 0.01 M buffer solution at pH 8 for one hour to ensure release of PVPON and then transferred to pH 5 to deswell the hydrogel films. After 30 min exposure, these films were dried with a gentle flow of nitrogen. Incorporation of gold nanorods was performed at pH 8 or 3. For that, the substrates with tethered films were first exposed to 0.01 M TRIS buffer solutions at certain pH values and then transferred to the solutions of gold nanorods in TRIS buffers whose pH was adjusted to either pH 8 or pH 3 by 0.01 M hydrochloric acid or sodium hydroxide solutions. After a certain time, the substrates with the LbL hydrogel films were taken from the gold nanorod solutions, washed with the buffers with an appropriate pH value, carefully dried with nitrogen, and their UV−vis absorbance spectra were taken.

For free-standing film fabrication and characterization, the (PMAA-Au NRs) films were prepared on top of a cellulose acetate (CA) sacrificial layer. A sacrificial CA layer was spin-cast from 0.5% CA solution in dioxane on a precleaned silicon wafer in accordance with the routine described earlier.[58,59] On top of it, $(PAH/PMAA)_3(PVPON/PMAA)_{20}$ layers were assembled with a spinning time of 20 s at 4000 rpm. Chemical cross-linking and incorporation of Au NR was performed as described above. After the fabrication, the hydrogel-Au NRs films were cut into $\sim 2 \times 2\ mm^2$ squares with a stainless steel syringe microneedle and released by exposure to acetone to dissolve the CA sacrificial layer. Drying these films without transfer resulted in significant wrinkling because of localized stresses. Thus, free floating LbL films were transferred directly to buffer solution at pH 5 from which they were picked up with various substrates and dried in air.

UV−Visible Spectroscopy (UV−Vis). UV−visible spectra of hydrogel-nanorod LbL films were recorded using a UV-2450 spectrophotometer (Shimadzu). Measurements were done on quartz substrates.

Atomic Force Microscopy (AFM). Surface morphology of the films was examined using AFM. AFM images were collected using a Dimension-3000 (Digital Instruments) microscope in the "light" tapping mode according to the established procedure.[60] For film thickness measurements, the edge of the film transferred on a silicon

(52) Zimnitsky, D.; Jiang, C.; Xu, J.; Lin, Z.; Tsukruk, V. V. *Langmuir* **2007**, *23*, 4509.
(53) Nikoobakht, B.; El-Sayed, M. A. *Chem. Mater.* **2003**, *15*, 1957.
(54) (a) Khanal, B. P.; Zubarev, E. R. *Angew. Chem., Int. Ed.* **2007**, *46*, 2195. (b) Khanal, B. P.; Zubarev, E. R. *J. Am. Chem. Soc.* **2008**, *130*, 12634.
(55) Kozlovskaya, V.; Shamaev, A.; Sukhishvili, S. A. *Soft Matter* **2008**, *4*, 1499.
(56) Kozlovskaya, V.; Sukhishvili, S. A. *Macromolecules* **2006**, *39*, 6191.
(57) Kharlampieva, E.; Erel-Unal, I.; Sukhishvili, S. A. *Langmuir* **2007**, *23*, 175.
(58) Jiang, C.; Markutsya, S.; Tsukruk, V. V. *Adv. Mater.* **2004**, *16*, 157.
(59) Zimnitsky, D.; Shevchenko, V. V.; Tsukruk, V. V. *Langmuir* **2008**, *24*, 5996.
(60) Tsukruk, V. V.; Reneker, D. H. *Polymer* **1995**, *36*, 1791.

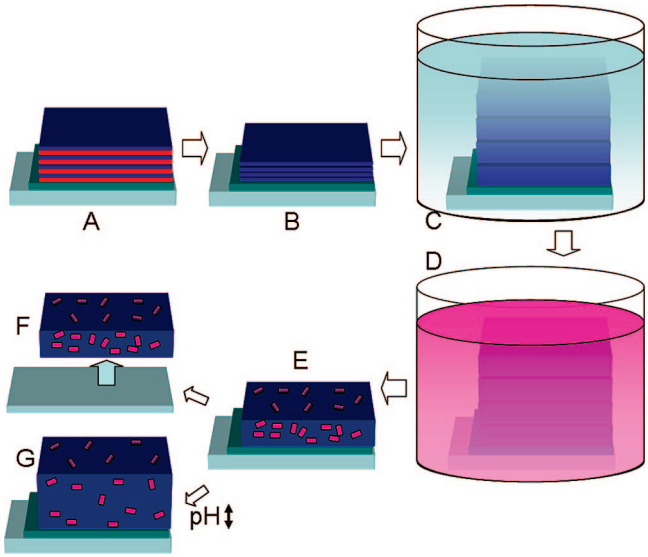

Figure 1. Preparation of pH-sensitive gold nanorod-containing LbL hydrogels: (A) SA-LbL self-assembly of hydrogen-bonded PVPON/PMAA films, (B) LbL PMAA hydrogel films after being cross-linked and PVPON was released from the hydrogel at basic pH, (C) swollen LbL PMAA hydrogel films. LbL PMAA hydrogel films after Au nanorods were loaded (D) and an excess of loosely bound nanorods was washed away by an appropriate buffer solution (E). Interaction of Au nanorods within the film can be controlled via pH changes (G) and the films can be released as free-standing membranes (F).

wafer was scanned and the image was analyzed with bearing analysis from NanoScope software to generate height histograms.

Transmission Electron Microscopy (TEM). TEM was performed on a JEOL 1200EX electron microscope operated at 100 kV. For gold nanorods, a drop of Au NR aqueous solution was cast onto carbon-coated copper TEM grids (Ted Pella) and allowed to dry. To analyze the nanorod-containing hydrogels, a piece of the free-floating film was picked with a copper grid and dried in air before TEM analysis.

Ellipsometry. Measurements of the film thickness and the refractive index in air and in a liquid cell were performed using a M-2000U spectroscopic ellipsometer (Woollam). All measurements were done at three angles of incidence of 65°, 70°, and 75°.

Contact Angle Measurements (CAM). Wetting of the hydrogel film surfaces was estimated by determining contact angles using optical measurements. Five microliters of water droplets were deposited on the LbL films at room temperature and the contact angles were automatically acquired by means of a CAM 101 (KSV Instruments).

Results and Discussions

Fabrication of LbL Hydrogel Films for Incorporation of Au Nanorods. Figure 1 schematically shows the procedure for stepwise preparation of ultrathin LbL hydrogel films with incorporated Au nanorods adapted in this study. First, hydrogen-bonded multilayers of PVPON/PMAA were formed using SA-LbL method. To investigate surface properties of these films, the hydrogen-bonded multilayers were constructed on silicon wafer surfaces from polymer solutions of various concentrations (Figure 1A). We found that there is almost no difference in the thickness for the films deposited from higher polymer concentrations of 0.5 mg/mL and 1.0 mg/mL (thicknesses of 3.3 and 3.5 nm per bilayer, respectively). However, further decrease in the

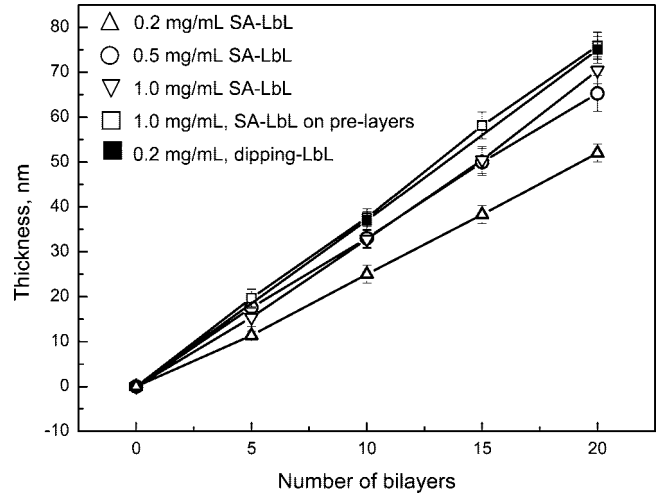

Figure 2. Thicknesses of PVPON/PMAA films built via the spin-assisted and dipping hydrogen-bonded LbL assembly from aqueous PVPON and PMAA solutions of various concentrations.

deposition solution concentration (0.2 mg/mL) resulted in 21% thinner films compared to those deposited from 0.5 mg/mL, with the bilayer thickness of 2.6 nm as one can see from Figure 2.

The film construction from 0.2 mg/mL polymer solutions using the dipping LbL method[61] is shown on the graph in Figure 2 for comparison. Our results on the film growth suggest that the films formed by hydrogen-bonded assembly via the spin-assisted method from diluted solutions are 1.5 times thinner than those produced via the dipping method. This difference may originate from different conditions under which such SA-LbL films are formed. Large shear forces due to high rotational speeds applied in this method could prevent the deposition of the saturated monolayer of polymer yielding the thinner films. The lower thickness of the polymer pair from the spin-assisted deposition when employing hydrogen bonding was also recently reported for hydrophobically modified poly(ethylene oxide)/poly(acrylic acid) (HM-PEO/PAA) films.[51] Similar trends were reported for electrostatically assembled PSS/PAH multilayer films constructed via spraying LbL versus conventional dipping LbL methods.[62,63] The slower multilayer growth of the sprayed films was also explained by nonequilibrium thicknesses of the resulted films due to a shorter contact time for the spraying method.

Robust attachment to a solid support is important for hydrogel pH-responsive films to ensure reliable studies on their swelling−deswelling related properties. For that purpose $(PVPON/PMAA)_{20}$ films were deposited on $(PAH/PMAA)_3$ thermally cross-linked prelayers. This approach allows for the formation of the reliable anchoring layer between the solid support and the LbL hydrogel film.[64] In this case, when PVPON/PMAA layers were spin-cast on $(PAH/PMAA)_3$-pretreated surfaces, we observed a slight increase in the film

(61) Sukhishvili, S. A.; Granick, S. *Macromolecules* **2002**, *35*, 301.
(62) Izquierdo, A.; Ono, S. S.; Voegel, J.-C.; Schaaf, P.; Decher, G. *Langmuir* **2005**, *21*, 7558.
(63) Porcel, C. H.; Izquierdo, A.; Ball, V.; Decher, G.; Vogel, J.-C.; Schaaf, P. *Langmuir* **2005**, *21*, 800.
(64) Kozlovskaya, V.; Kharlampieva, E.; Mansfield, M. L.; Sukhishvili, S. A. *Chem. Mater.* **2006**, *18*, 328.

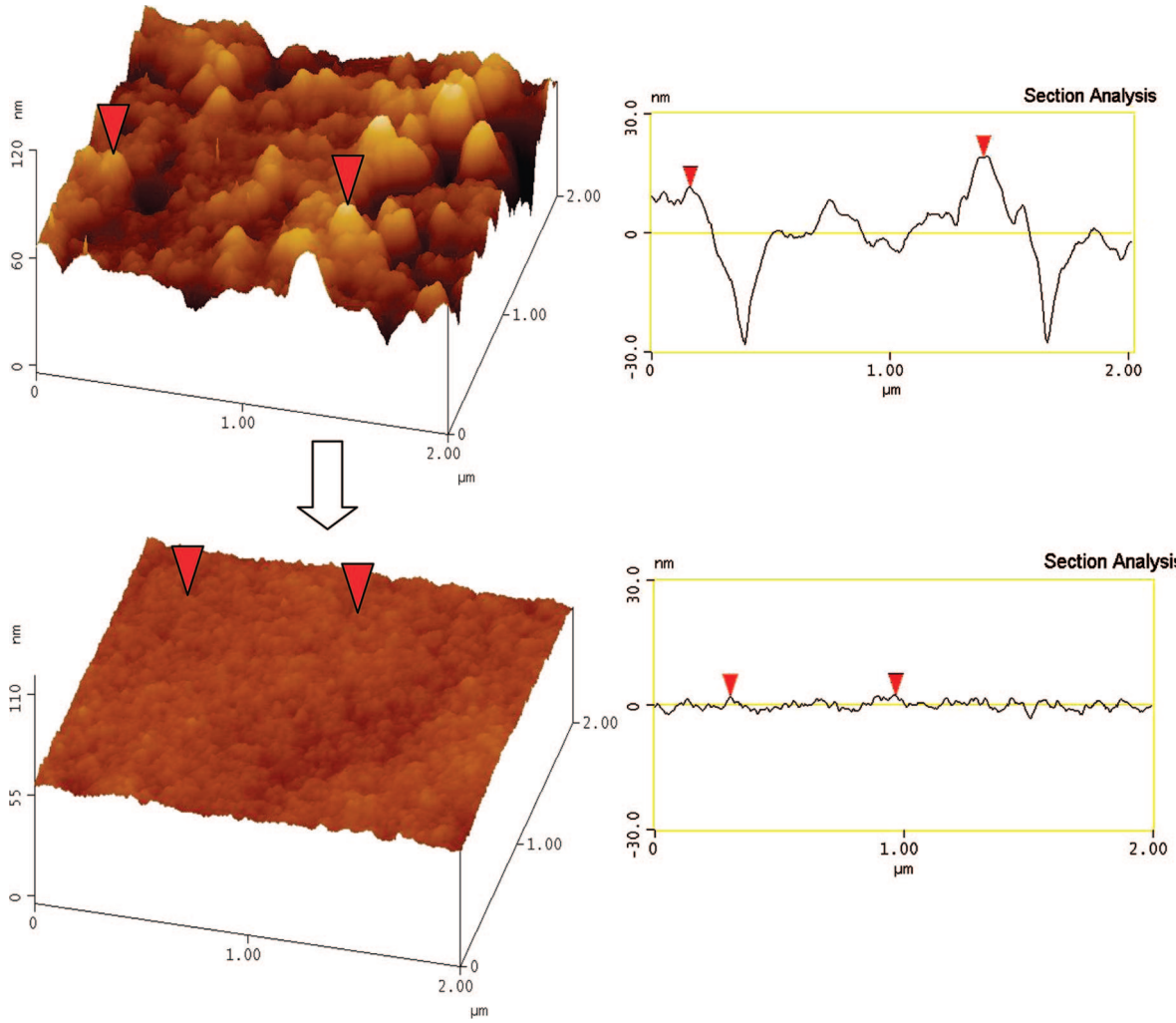

Figure 3. AFM images and cross-sections of a hydrogen-bonded $(PVPON/PMAA)_{20}$ film deposited at pH 2.5 from 1 mg/mL buffer solutions via spin-assisted LbL (top) and of a hydrogel $(PMAA)_{20}$ film produced by chemical cross-linking of a SA-LbL $(PVPON/PMAA)_{20}$ film and dried from pH 5 (bottom). *Z*-scale is 30 nm for both images. Markers show the areas along which the cross-sections were made.

thickness with 3.8 nm per bilayer for $(PAH/PMAA)_3(PVPON/PMAA)$ films spin-cast from 1.0 mg/mL versus 3.5 nm per bilayer for pure (PVPON/PMAA) layers spin-cast from the same concentration solutions. The larger thickness in the former case can be explained by the fact that the hydrogen-bonded multilayer growth and their thickness values can be strongly affected by the proximity of charged surfaces imposing strong limitations on deposition conditions.[65] The electrostatically bound $(PAH/PMAA)_3$ prelayers help to eliminate such substrate effects and result in thicker films.

It is interesting to note that although the incremental bilayer thickness for PVPON/PMAA films varied for that deposited from diluted and concentrated polymer solutions, the molar excess of PMAA units over PVPON remained approximately the same for all studied deposition solution concentrations and was close to 2.3. This value is in good agreement with those reported earlier for hydrogen-bonded PVPON/PMAA (2.1 times)[61] and poly(*N*-vinylcaprolactam)/PMAA multilayers (1.6 times)[66] fabricated via the conventional dipping LbL assembly.

To yield a pH-responsive polymer matrix of the largest thickness useful for incorporation of 25 nm diameter gold nanorods, the hydrogen-bonded (PVPON/PMAA) platform was built up from 1.0 mg/mL polymer solutions on the prelayer-treated surfaces and then chemically cross-linked as reported previously (Figure 1B).[57] Specifically, EDA was used in this work as a bifunctional cross-linker for $(PMAA)_{20}$-layered hydrogel films. After exposure of the films to pH 8 and release of the neutral polymer out of the produced (PMAA) hydrogel matrix the film thickness decreased by 30% meaning the complete release of PVPON.[56] Figure 3 demonstrates cross-sectional analysis of the $(PAH/PMAA)_3(PVPON/PMAA)_{20}$ hydrogen-bonded platform formed at pH 2.5 via SA-LbL method before and after cross-linking was performed. Overall smoothening of the LbL surface occurred due to dissolution of the previously formed hydrogen-bonded complexes between the poly(carboxylic acid) and PVPON and overall polymer matrix extension due to increased hydrophilicity of the polyacid chains after PVPON was released.[67] Furthermore, even larger decrease in the hydrogel surface roughness was observed when SA-LbL $(PMAA)_{20}$ films were dried from either pH 8 or pH 3.

(65) Kozlovskaya, V.; Yakovlev, S.; Libera, M.; Sukhishvili, S. A. *Macromolecules* **2005**, *38*, 4828.
(66) Kharlampieva, E.; Kozlovskaya, V.; Tyutina, J.; Sukhishvili, S. *Macromolecules* **2005**, *38*, 10523.
(67) Kozlovskaya, V.; Sukhishvili, S. A. *Macromolecules* **2006**, *39*, 5569.

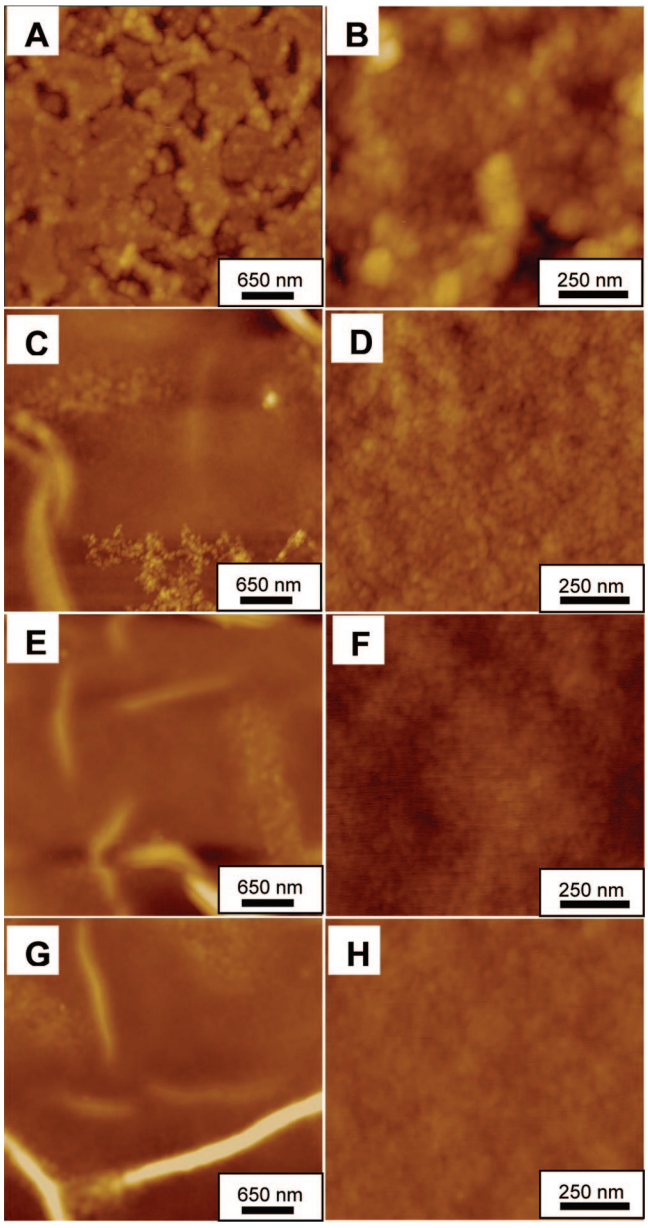

Figure 4. AFM images of the LbL hydrogen-bonded $(PVPON/PMAA)_{20}$ film spin-coated from 1 mg/mL aqueous solutions at pH 2.5 (A, B). A cross-linked $(PMAA)_{20}$ film at $(PAH/PMAA)_3$-treated silicon wafers dried from pH 5 (C,D), from pH 8 (E, F), or from pH 3 (G, H). Z-range is 150 nm for A, C, E, and G and 30 nm for B, D, F, and H.

Root-mean-square microroughness (rms) measured at $(1 \times 1)\ \mu m^2$ area for 20-layer cross-linked (PMAA) film at $(PAH/PMAA)_3$-treated silicon wafer surfaces dried from pH 8 and from pH 3 were 0.8 and 0.9 nm, respectively compared to 3.6 nm for the initially deposited films and 1.3 nm for $(PMAA)_{20}$ at pH 5 (Figure 4). Lower microroughness of the cross-linked films at pH 8 and pH 3 reflected additional extension of the polyacid matrix caused by its electrostatic ionization under these conditions. The larger $(5 \times 5)\ \mu m^2$ scans of the (PMAA) hydrogel films revealed the appearance of larger scale wrinkles on the hydrogel surfaces (Figure 4). Their presence in the dried cross-linked films can be attributed to the restricted 3D swelling of the tethered hydrogel LbL films which causes localized compressive stresses.

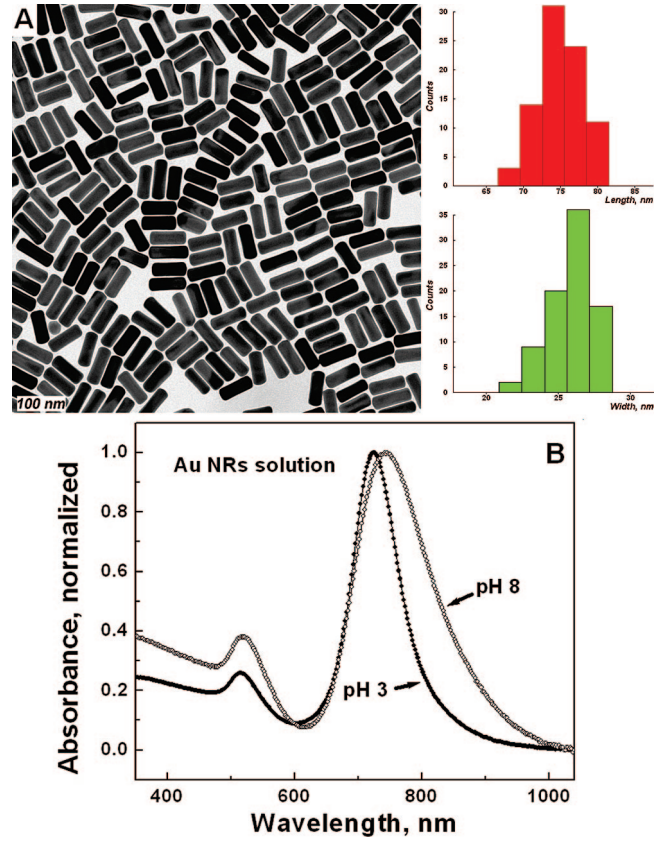

Figure 5. A: TEM image of CTAB-stabilized gold nanorods cast from solution on a carbon-coated copper TEM grid and their size distribution in length (top) and in width (bottom). B: Normalized UV−visible spectra from solutions of CTAB-stabilized gold nanorods exposed to pH 3 (filled circles) and pH 8 (open circles) buffers.

Incorporation of Au Nanorods within Swollen LbL Hydrogel Films. From TEM analysis of the nanorods utilized here, the average aspect ratio of the synthesized gold nanorods was $L/W = 3$ with the width and length of 25 ± 3 nm and 74 ± 7 nm, respectively (Figure 5A). The UV−visible spectra show two distinct absorption maxima at pH 3 and 8 (Figure 5B). The absorbance peak around 515 nm corresponds to the transverse plasmon oscillations and the peak with the higher intensity is responsible for the longitudinal plasmon resonance peak.[68] The initial gold nanorod solution (pH = 3) shows a longitudinal absorbance peak maximum of 725 nm (filled circles in Figure 5B). A red-shift to 745 nm and broadening of the peak with some reduced intensity occurred when the pH of the nanorod dispersion was adjusted to pH 8. The red-shift of the longitudinal plasmon band with no significant change in transverse plasmon peak position can be related to modest aggregation of gold nanorods in solution.[69]

The reversibility in UV absorbance in response to pH was observed during the first two pH adjustments and gradually deteriorated with the subsequent pH cycles. These changes in absorption of the solution are caused by aggregation of the nanorods due to dilution during pH adjustments resulting in subsequent gradual removal of CTAB molecules respon-

(68) Jain, P. K.; Eustis, S.; El-Sayed, M. A. *J. Phys. Chem. B* **2006**, *110*, 18243.
(69) Joseph, S. T. S.; Ipe, B. I.; Pramod, P.; Thomas, K. G. *J. Phys. Chem B* **2006**, *110*, 150.

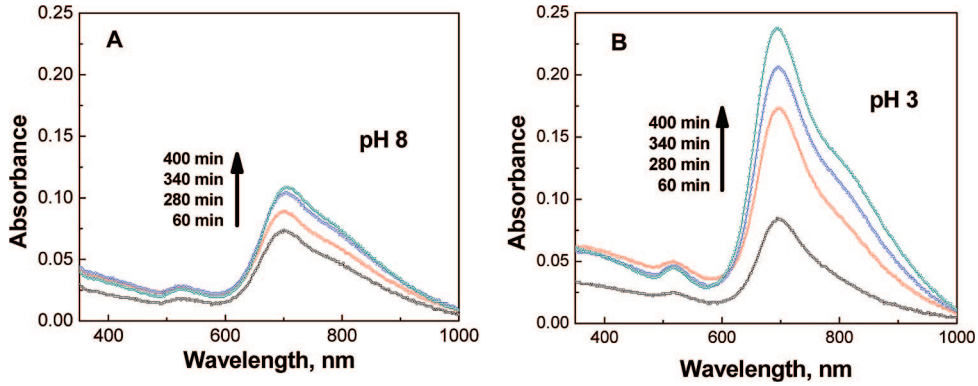

Figure 6. Absorbance of $(PAH/PMAA)_3(PMAA)_{20}$ hydrogel films loaded with gold nanorods at pH 8 (A) and at pH 3 (B) for different periods of time.

Scheme 1. Internal Structure of the Hydrogel Film at pH 3 (left) and pH 8 (right) before Loading of Gold Nanorods (middle) into the Swollen LbL Films

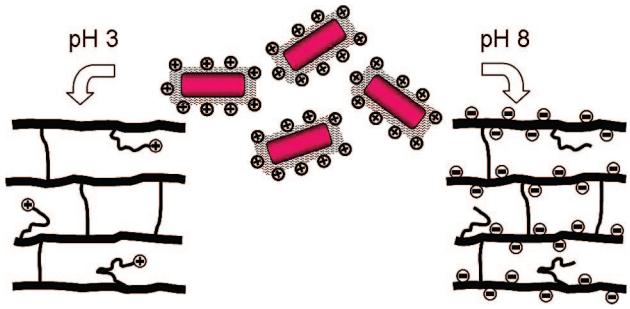

sible for stabilization of the nanorods. Finally, the precipitation of the gold particles occurred upon standing of the solution at pH 8 for longer than 15 h. Similarly, Kim and co-workers recently demonstrated that repetitive washings of free gold nanorods caused irreversible aggregation of the nanorods due to decreasing the minimum amount of the surfactant molecules necessary for maintaining colloidal stability of the nanorods in solution.[70]

The dependence of the SPR wavelength on the environment around gold nanoparticles can be the convenient parameter useful to monitor changes induced by the variation in environmental pH or chemical composition of the media.[71] Thus, change in the surroundings can affect interparticle interactions resulting in a strong shift in the surface plasmon resonance of the nanorods easily monitored by UV−visible spectroscopy. In such a case, the gold nanorods can be considered as optical tags designated to follow the environmental changes.

The gold nanorods exploited in this work were positively charged owing to the stabilizing bilayer of CTAB.[72] Therefore, a swollen LbL hydrogel was exposed to Au nanorod solution at pH 8 to favor electrostatically driven incorporation of the nanorods within the hydrogel film (Figure 1C,D). Figure 6A shows the evolution of the UV−visible spectrum of the quartz-attached $(PAH/PMAA)_3(PMAA)_{20}$ film upon gradual accumulation of the nanorods from solution within the LbL film at pH 8. The spectra exhibit two absorbance maxima associated with the presence of the nanorods similar

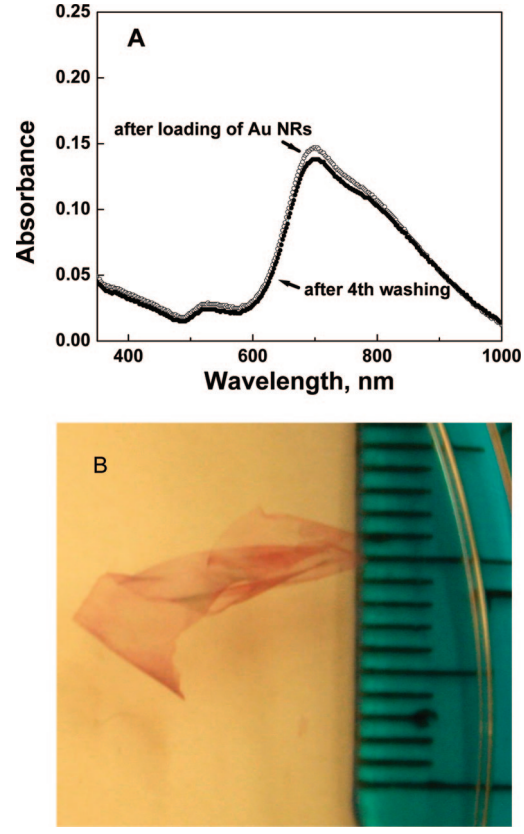

Figure 7. A: UV−vis absorption spectra of the $(PAH/PMAA)_3(PMAA\text{-}Au)_{20}$ films loaded at pH 8 for 15 h, as produced (open circles) and after four washings in pH 8 buffer solution (filled circles). B: Optical image of $(PMAA\text{-}Au)_{20}$ film freely floating in water; the ruler shows a scale in millimeters.

to those in solution (Figures 5B and 6). The longitudinal absorbance peak at 701 nm becomes more intense with increasing loading time with the slight red shift developing after approximately 5 h of loading. Such gradual gain in the intensity of the peak is attributed to the increasing number of gold nanorods included into the hydrogel film due to electrostatic interactions between negatively charged COO^- groups present in the swollen cross-linked matrix and the positively charged CTAB corona around Au NRs (Scheme 1, right). Interestingly, in case of the SA-LbL for $(PVPON/PMAA)_5Au$ NRs$(PMAA/PVPON/PMAA)_5Au$ NRs at pH 4, almost no nanorods could be deposited between the hydrogen-bonded stacks implying poor electrostatic interactions between CTAB-stabilized Au nanorods and slightly negatively

(70) Koo, H. Y.; Choi, W. S.; Kim, D.-Y. *Small* **2008**, *7*, 42.
(71) Tokareva, I.; Tokarev, I.; Minko, S.; Hutter, E.; Fendler, J. H. *Chem. Commun.* **2006**, 3343.
(72) Nikoobakht, B.; El-Sayed, M. A. *Langmuir* **2001**, *17*, 6368.

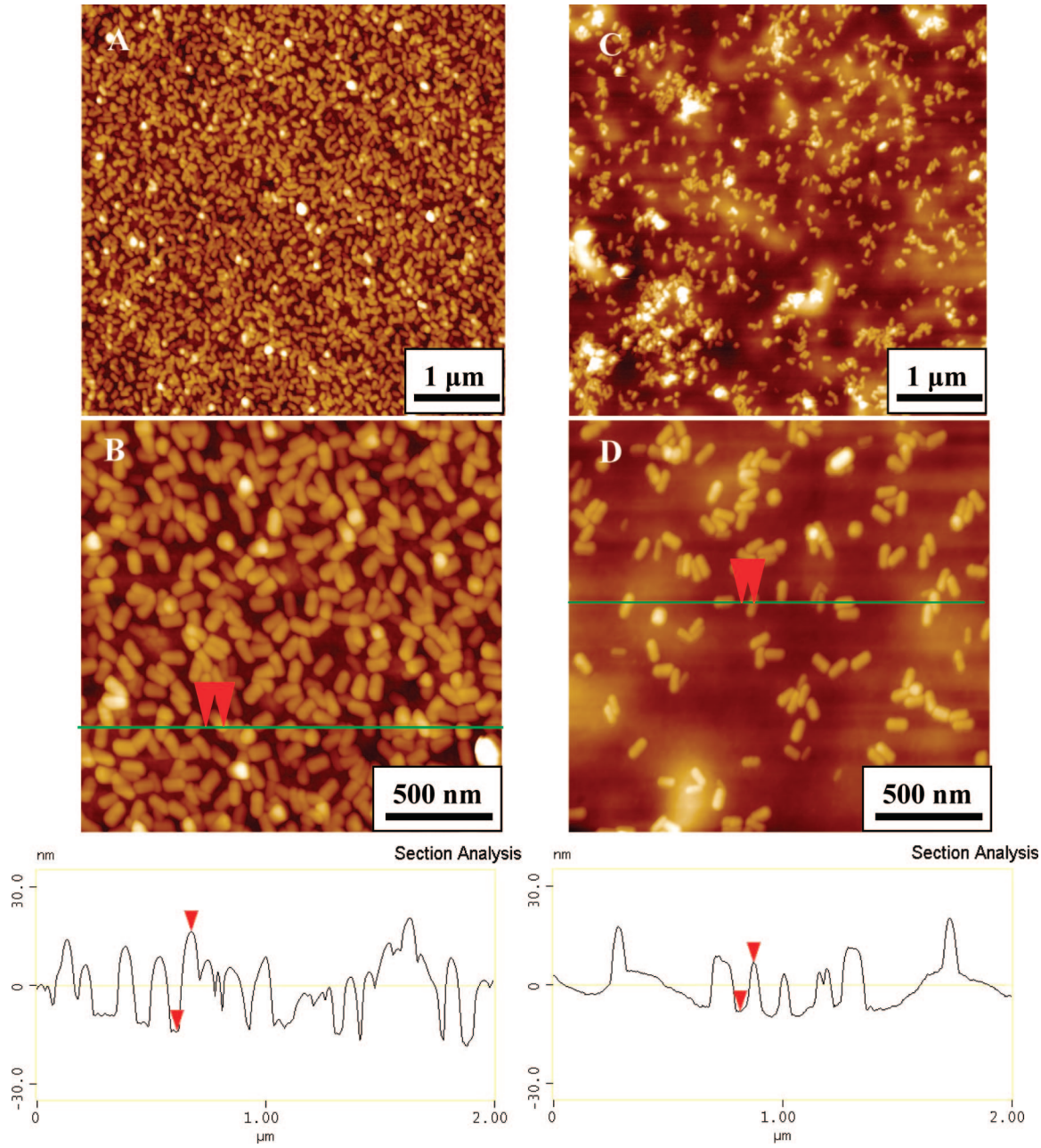

Figure 8. AFM images of the $(PAH/PMAA)_3(PMAA)_{20}$ hydrogel films loaded with Au NRs at pH 3 (A, B) and at pH 8 (C, D) for 10 h, washed with appropriate pH solutions and subsequently dried with a stream of nitrogen.

charged PMAA. Similarly, only a small portion of CTAB-stabilized gold nanorods was initially adsorbed onto the polyelectrolyte surface of $(PAH/PSS)_n$ capsules but later they were easily detached from the PAH/PSS multilayers upon the following washings.[70]

Such poor surface interaction of CTAB-stabilized Au nanorods with oppositely charged polyelectrolyte-coated surfaces was explained also by possible adsorption of free CTAB molecules from the nanorods solution. When adsorbed on negatively charged polyelectrolytes, these CTAB bilayers inhibited further adsorption of CTAB-coated gold nanorods due to same charge repulsions.[73] In our case, there was a negligible decrease in overall peak intensity after four-time washing of the loaded hydrogel with pH 8 buffer solution implying that most of the nanorods were electrostatically bound within the hydrogel film (Figure 7A). The shoulder at 780 nm after short loading indicates the initial presence of some aggregated nanorods caused by the necessity to adjust pH of the nanorods solution to pH 8.

We also explored the possibility to incorporate Au nanorods into the $(PMAA)_{20}$ hydrogel film swollen at pH 3 (Scheme 1, left). Swelling of the film at this pH is caused by mutual repulsions of positively charged amino groups from the one-end attached cross-linker molecules.[56] Due to the same charge of Au nanorods and the hydrogel film, no nanorod inclusion could be anticipated. Surprisingly, we observed a steady increase in the peak intensity of the longitudinal plasmon band at ~700 nm with increasing loading time finally saturating after 7 h (Figure 6B). The shoulder at longer wavelengths becomes more pronounced

(73) Rutland, M. W.; Parker, J. L. *Langmuir* **1994**, *10*, 1110.

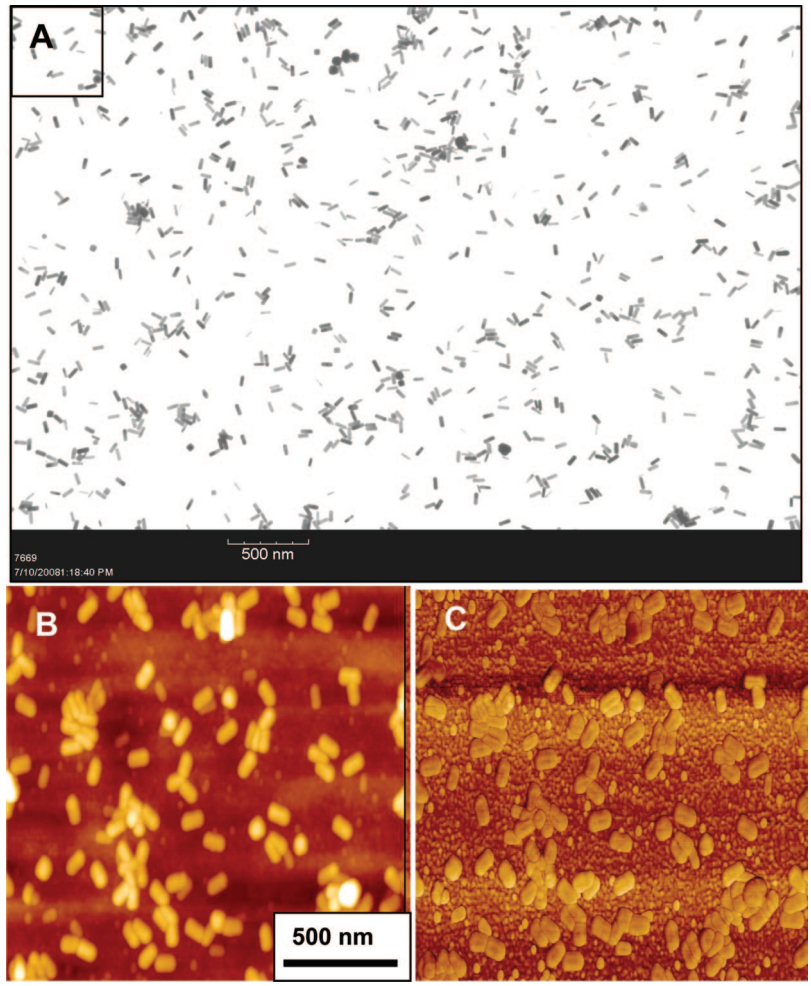

Figure 9. TEM image of the (PMAA-Au NRs)$_{20}$ hydrogel film loaded at pH 8 for 15 h (A). The loaded film was released into water, picked up with TEM grid and dried in air. AFM topography (left) and phase (right) images of (2 × 2) μm^2 surface area of the (PMAA-Au NRs)$_{20}$ film (B and C, respectively); *z*-scale is 100 nm (left) and 50° (right).

with larger loading times implying an increased agglomeration of the nanorod aggregates with time. We suggest that in the case of loading of the nanorods into the hydrogel film at pH 3, positively charged amino groups can deprive gold nanorods of the positively charged CTAB corona through repulsive interactions and induce spontaneous precipitation of the nanorods within the swollen hydrogel film. Note that there is also a possibility of Au nanorods interactions with the present amino groups due to high affinity of gold to amino groups.[74]

AFM imaging of the films loaded at pH 8 and 3 well correlated with the UV−visible spectroscopy results (Figure 8). It is clearly seen that the number of the nanorods included in the (PMAA)$_{20}$ film at pH 8 for 10 h is less than that at pH 3. This difference is most probably caused by free CTAB molecules from the nanorod solution at pH 8, which can be electrostatically attracted to the swollen negatively charged hydrogel film along with the CTAB-coated nanorods. Such free CTAB molecules can block some of the available COO^- binding sites and prevent the LbL film from overloading with the nanorods.

Cross-sectional analysis of the surface topography reveals that the gold nanorods which are seen on the hydrogel surface are partially embedded within the films both loaded at pH 8 and pH 3 (Figure 8). An average height of the nanorods obtained from cross-sectional analysis of the (PMAA-Au NRs)$_{20}$ film was 15 ± 3 nm (Figure 9). We suggest that this loading was possible because it was performed into a highly swollen LbL hydrogel with thickness much higher than the diameter of the nanorods. Even if dry thickness of the produced (PMAA)$_{20}$ hydrogel films measured by ellipsometry was 54 ± 3 nm, after exposure to buffered solutions at pH 5 and pH 8, the hydrogel thickness increased twofold yielding 106 and 202 nm, respectively. These values were in very good agreement with our previous work performed on PMAA hydrogel films.[57,64] As has been suggested, the swelling of the hydrogel film was due to hydration of the polymer networks and their further ionization along with the osmotic pressure of ions.

Surface Properties of (PMAA-Au NRs) Hydrogel LbL Films. TEM analysis of the free-standing (PMAA-Au NRs)$_{20}$ film loaded with gold nanorods at pH 8 (shown in Figure 7B) and transferred on the TEM grid revealed the embedded nanorods (Figure 9A). The low contrast between free hydrogel surface and surfaces of most of gold nanorods on

(74) Wangoo, N.; Bhasin, K. K.; Mehta, S. K.; Raman Suri, C. *J. Colloid Interface Sci.* **2008**, *323*, 247.

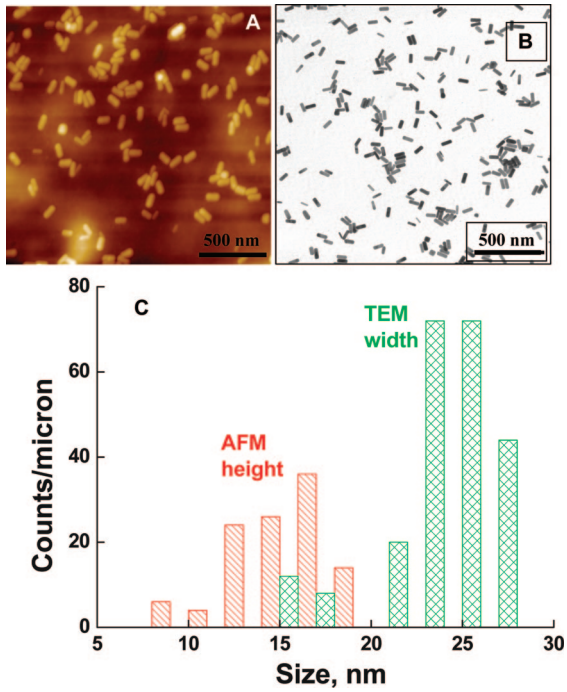

Figure 10. AFM and TEM images of (2 × 2) μm^2 surface area of the $(PMAA\text{-}Au\ NRs)_{20}$ film (A and B, respectively); *z*-scale for the AFM image is 100 nm. C: Histograms of the height of the embedded gold nanorods from AFM images and their width calculated from the TEM images of (2 × 2) μm^2 surface area, respectively. Total number of counts corresponds to the number of nanorods visible within selected surface area.

corresponding phase images obtained in very light tapping mode indicates that the nanorods are mostly covered by the hydrogel material as can be concluded from the analysis of the mechanism of interaction between AFM tip and the biphasic materials (Figure 9B,C).[75] Indeed, considering that, under light tapping mode, phase contrast is mainly controlled by the adhesive properties of the surface, we can conclude that the hydrogel material covers most of gold nanorods visible in this image. This result suggests that a significant fraction of gold nanorods is partially embedded into the hydrogel film and not just tethered to its surface.

Indeed, the number of gold nanorods obtained from 2 μm × 2 μm surface area from TEM analysis was calculated to be two times larger that the number of the topmost nanorods obtained from AFM images from the same surface area (Figures 10A,B). This difference confirms the inclusion of the nanorods within the hydrogel with at least half of them buried deep inside hydrogel films, well beneath the topmost hydrogel layer. In addition, the apparent height of the topmost gold nanorods estimated from AFM images is about twice lower than that estimated from TEM images indicating that even nanorods tethered to the surface are partially (50%) embedded into supporting material (Figure 10C). Finally, the analysis of projectional dimensions of gold nanorods demonstrates that more than 90% of all them are lying within the plane of the films with very few nanorods standing in vertical orientation (Figure 8). Apparently, such in-plane preferential arrangement is caused by the spatial constraints imposed by the limited thickness of dry ultrathin hydrogel films comparable with the length of the nanorods.

Table 1. Contact Angles of $(PMAA)_{20}$ and $(PMAA\text{-}Au\ NRs)_{20}$ Hydrogel Films in Their Swollen (pH 8 and pH 3) and Deswollen (pH 5) States[a]

	pH 8	pH 5	pH 3
$(PMAA)_{20}$	<10°	<10°	38 ± 2°
$(PMAA\text{-}Au\ NRs)_{20}$	32 ± 3°	52 ± 3°	46 ± 2°

[a] Gold nanorods were loaded into the film at pH 8 for 10 h.

The lowest contact angle for $(PMAA\text{-}Au\ NRs)_{20}$ was found to be 32 ± 3° after the film was dried from pH 8 (Table 1). This value reflects increased hydrophilicity of the film because of the ionization of the surface carboxylic groups which is similar to the trend observed for the bare $(PMAA)_{20}$ film. The contact angle increase for both $(PMAA)_{20}$ and $(PMAA\text{-}Au\ NRs)_{20}$ swollen films at pH 3 (38 ± 2° and 46 ± 2°, respectively) reflected increased hydrophobicity of the uncharged poly(carboxylic acid) chains compared to that at higher pH. Higher hydrophobicity of PMAA was reported to yield hydrophobic clusters within PMAA chains in aqueous solutions at low pH values.[76,77] On the other hand, at pH 5 the $(PMAA\text{-}Au\ NRs)_{20}$ film is efficiently neutral[57] and deswollen, which results in the highest value for the contact angle of 52° ± 3°. The observed changes in the surface properties of the hydrogels loaded with the gold nanorods also suggest their presence in the polymer matrix.

Optical Properties of (PMAA-Au NRs) Hydrogel Films. Figure 11A shows UV−visible spectra of the $(PMAA\text{-}Au\ NRs)_{20}$ hydrogel films at different pHs. The longitudinal SPR peak changes its position in response to changes in the pH of the environment. The plasmon peak blue-shifts by 21 nm after the loaded hydrogel film was transferred from pH 8 to pH 5. Such a shift corresponds to the increased coupling between nanorods caused by the closer side-by-side assembly of the nanorods as suggested by theoretical consideration.[68] The more intense coupling of the nanorods in this case occurred when they closely assemble in response to deswelling of the hydrogel matrix after the pH decrease. Using the literature data on the extinction efficiency of gold nanorods with aspect ratio of 4 [68,78] in a side-by-side orientation, we estimated the distance between the interacting nanorods within the loaded film to be close to 30 nm.

It is worth noting that a small red-shift in the transverse SPR peak (4 nm) was also observed after the pH change from 8 to 5. This result also confirms the increased side-by-side interactions of the nanorods upon the hydrogel deswelling and agrees with the literature results. [69,79] The changes in the peak position for the $(PMAA)_{20}$ hydrogel films loaded at pH 3 showed only a slight shift of 6 nm to higher energies in response to lowering pH from 8 to 5 which is most likely because of high degree of the nanorods loading (not shown). We hypothesize that such close assembly of the nanorods in the hydrogel film did not allow for pronounced changes in the internanorod distance and therefore resulted in a small shift in the longitudinal plasmon band.

(75) Luzinov, I.; Julthongpiput, D.; Tsukruk, V. V. *Macromolecules* **2000**, *33*, 7629.
(76) Bednáø, B.; Trnená, J.; Svoboda, P.; Vajda, S.; Fidler, V.; Prochazka, K. *Macromolecules* **1991**, *24*, 2054.
(77) Soutar, I.; Swanson, L. *Macromolecules* **1994**, *27*, 4204.
(78) Lee, K.-S.; El-Sayed, M. A. *J. Phys. Chem. B* **2005**, *109*, 20331.
(79) Thomas, K. G.; Barazzouk, S.; Ipe, B. I.; Joseph, S. T. S.; Kamat, P. V. *J. Phys. Chem. B* **2004**, *108*, 13066.

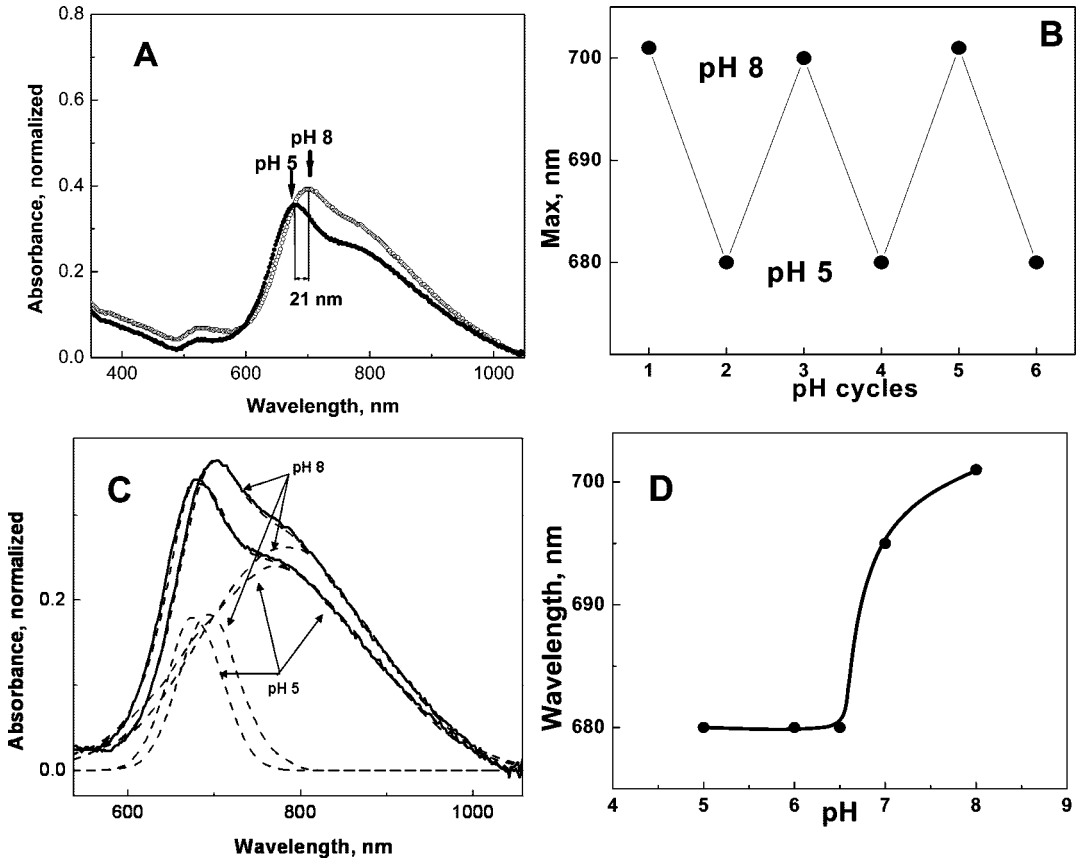

Figure 11. A: Absorbance of $(PMAA\text{-}Au\ NRs)_{20}$ hydrogel film (with Au nanorods loaded into the hydrogel film at pH 8 for 15 h) exposed to pH 8 (open circles) and to pH 5 (filled circles). B: Reversible variations in the absorbance maximum of the hydrogel film from 701 to 680 nm in response to pH change from 8 to 5, respectively. C: Absorbance of $(PMAA\text{-}Au\ NRs)_{20}$ hydrogel film exposed to pH 8 and to pH 5. Peaks obtained from the fitting analysis of the original spectra (solid lines) are shown with dashes. D: The evolution of the longitudinal SPR peak position from pH 5 to 8.

The pH-dependent shifts of the SPR peaks were highly repeatable as one can see from the Figure 11B. Alternate variations between the pH values of 5 and 8 with the exposure time for 15 min in each solution resulted in the reversible change of the plasmon peak between 680 and 701 nm. Deconvolution analysis of the longitudinal plasmon band yielded the presence of two peaks at 692 and 783 nm. Upon the pH change from 8 to 5, these peaks are consistently shifted to 672 and 768 nm, respectively (Figure 11C). We attribute the former peak to the presence of individual Au nanorods loaded into the PMAA hydrogel film while the latter can be associated with the aggregated nanorods whose existence is confirmed by the AFM studies (Figure 8). The consistent shifts of the longitudinal plasmons may reflect an increase in the refractive index within the (PMAA) hydrogel films.[80,57] In fact, the refractive index of hydrogel films (without nanorods) changed from 1.36 at pH 8 to 1.43 at pH 5 as was measured with spectroscopic ellipsometry for films in the swollen state directly in a liquid cell.

We also examined how the plasmon absorbance peak changes in response to stepwise variations between the target pH values. We have previously shown that swelling transition in cross-linked PMAA hydrogels occurs in the pH range of 6−6.5 (with reported pK_a values of PMAA ∼ 6).[56] Indeed, a sharp transition in the absorbance maximum occurs around pH 7 (Figure 11D). We suggest that the slightly increased pH threshold for the detected conformational changes is due to the presence of positively charged CTAB-coated gold nanorods. At neutral pH, Au nanorods contribute to the ionic NH_3^+/COO^- cross-linking which coexists with covalent cross-links within the film and therefore delay the swelling of the hydrogel film.

Conclusions

We report on a straightforward fabrication of the optically responsive ultrathin membranes useful for monitoring membrane swelling/deswelling changes in the biologically important pH range from 5 to 8. The ultrathin, 55 nm membranes were fabricated by inclusion of the gold nanorods into the swollen cross-linked $(PMAA)_{20}$ LbL hydrogel films through electrostatic interactions. We demonstrated that in contrast to the majority of the sensing methods reported in the literature which rely mostly on the quenching effects when the intensity decrease is monitored upon the environmental change event, pH-induced swelling/deswelling of the reported $(PMAA\text{-}Au\ NRs)_{20}$ membranes can be easily tracked by monitoring shifts in the longitudinal SPR peak of gold nanorods. We show that pH-induced deswelling of the $(PMAA\text{-}Au\ NRs)_{20}$ film causes a significant blue-shift of the plasmon band by 21 nm, which reflects the increased side-by-side interactions of gold nanorods and an increase

(80) Pristinski, D.; Kozlovskaya, V.; Sukhishvili, S. A. *J. Opt. Soc. Am. A* **2006**, *23*, 2639.

in the refractive index within the hydrogel film with the pH decrease from 8 to 5.

We suggest that the longitudinal SPR peak of gold nanorods is more suitable for monitoring pH-induced changes within the membranes than the transverse SPR band for nanorods or for gold nanoparticles due to its stronger intensity and higher sensitivity to the environmental conditions. Importantly, due to the stronger interactions among gold nanorods within highly loaded hydrogel films the substrate precoating with gold is not required to yield large SPR response to pH changes. In contrast with most of known pH responsive materials which rely on pH-triggered change in the intensity of photoluminescence or plasmon bands, the responsive structures suggested here cause pH-triggered and very significant shift in easily detectable plasmon resonance bands. Additionally, it is worth noting that these ultrathin hydrogel films are strong enough to be released from the substrates yielding free-floating films, and thus they can be utilized as stand-alone pH responsive membranes. Moreover, these hydrogel LbL films can be further transferred to other microfabricated supports and utilized in a variety of sensing applications.

Acknowledgment. This work was supported by funding provided by NSF-CBET-NIRT Grant 0650705 and Air Force Office of Scientific Research Project No. FA9550-08-01-0446. E.R.Z. acknowledges the additional financial support by NSF CAREER Award (DMR-0547399), Robert A. Welch Foundation (C-1703), and Alfred P. Sloan Foundation.

CM8023633